Targeted Opportunities for Graphene Enhanced Water Security and Infrastructure Materials

Chris S. Griggs, Sarah Grace Zetterholm, Mine G. Ucak-Astarlioglu, Jesse D. Doyle, and Luke Gurtowski
US Army Engineer Research and Development Center, 3909 Halls Ferry Road,
Vicksburg, MS 39180
USA

Chris.S.Griggs@usace.army.mil

ABSTRACT

Emerging technologies, such as graphene, are driving fundamental changes in "materials-by-design" concepts. As these technologies mature, the new access to graphene and "graphenic" carbons at viable scale and cost advance the science beyond computational predictions and into synthesis and characterization of real-world applications. Our research focuses on the graphene enhancement of conventional bulk materials and processes to harness graphene functionality to produce new classes of ultra-materials through small process changes in concrete, asphalt, and water treatment chemistry. New knowledge, strategies, and expertise in handling and modifying graphene-platforms can capitalize on targeted opportunities for enhanced performance and life cycle considerations of structural assets and water infrastructure. Here we show the direct use of graphene as a rational interface for functional coatings. Although non-covalent interactions typically rely on computational methods for mechanistic insight, Nuclear Magnetic Resonance (NMR) titrations were performed to probe primary interfacial interactions between graphene and the conventional host materials. Interactions between the aromatic rings and graphene sp2 orbitals are the dominant interactions and can be exploited to impart graphene functionality to conventional materials though π bonding. Current projects include design and development of "tunable" graphene; varying particle size, surface area, and morphology to match the desired performance. Key to advancing the technologies is understanding the non-covalent interactions of graphene itself and its compatibility with polymers, binders, and other commercially available products. This paper will highlight novel mechanisms of selective water purification, > 150% extended lifecycles of asphalt binders, and > 80% strength increase of concrete through graphene modifications.

Keywords: *graphene, adsorption, non-covalent, sp2 carbon*

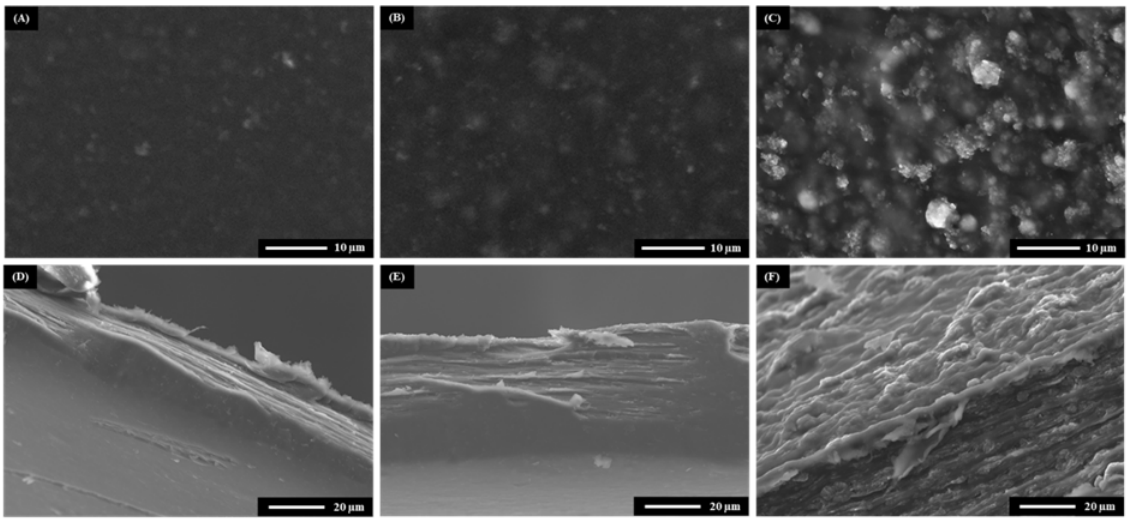

1.0 INTRODUCTION

As graphene research continues to progress, potential applications are evolving from theoretical predictions and into real-world commercial usage. However, key to advancing graphene Technology Readiness Levels (TRLs) for military requirements is overcoming scalability challenges. Even as graphene production increases at viable cost and scale, technical barriers exist in graphene dispersion and interface with the host materials. Essential to advancing the technologies is understanding the non-covalent interactions of graphene itself and its compatibility with polymers, binders, and other commercially available products [1]. Therefore, there is a requirement for design and development of "tunable" graphene – varying particle size, surface area, and morphology to match the desired performance. Two major military application spaces identified as ideal candidates for graphene enhancement are development of a selective water treatment media for filtration systems, and next generation construction materials for Force Projection.

Water security is a fundamental element of the readiness and resilience of the U.S. Army. Thus, new directives for both installation and operational water resiliency have been established. Water scarcity is emerging as a risk multiplier in operational environments, and resupply constitutes high demand signatures and logistical burdens. Although not commonly practiced, recycling and reuse of water may be needed to efficiently maximize use of water sources. For potable reuse, military guidelines can be found in USACHPPM 2001 Proposed Water Quality Criteria for Recycled Gray Water for Force Provider and TB MED 577 [2], [3]. Preventive Medicine (PM) personnel must approve water for use; therefore, Reverse Osmosis (RO) Water Purification System technologies are often used as a technology requirement in military field exercises for rapid treatment and reuse capabilities for rejection of salts and low molecular weight organic substances [3]. Although RO appears to be an effective safety barrier to ensure adequate removal for most contaminants, including micropollutants, it is energy intensive.

Broad spectrum carbonaceous materials used for water filtration, such as Granular Activated Carbon (GAC), are limited to only surface-area-based sorption and are subject to competing organic co-contaminants. Immediate improvements to be gained using graphene are tailored removal mechanisms specifically for interaction with emerging contaminants molecules, such as Personal Care and Pharmaceutical Products (PCPP), and toxic metabolites of cyanobacteria that are challenging to detect and remove in the field. Based on the sp2-hybridized carbon system, the concept of harnessing π-π type interactions for contaminant removal can be used for enhanced kinetics and adsorptive capacities. By tuning the porosities and higher surface aromatic content of graphene, rapid diffusion into mesopores through π-π interactions can decrease the size of a deployable filtration system. Although GAC has a larger total surface area than graphene, adsorption is limited by interparticle diffusion and lack of aromatic groups on the surface [4]; therefore, it can be necessary to have a much larger carbon bed volume of amorphous carbons to produce the same removal capability as graphene for certain contaminants [5].

Due to the multifunctional nature of graphene, its properties can also be integrated for next generation construction materials. The addition of graphene to bulk construction materials including asphalt concrete (AC) and Portland Cement Concrete (PCC), has potential to greatly improve their properties. Both Graphene nano-Platelets (GnPs) and Graphene-Oxide (GO) have been incorporated into AC. Graphene, being pure carbon, is highly compatible with organic hydrocarbons in asphalt cement, making AC an ideal candidate for graphene modification. Addition of GnP to asphalt cement has shown potential for significant, greater than 100%, improvement in low temperature fracture resistance. Graphene modification acts as an aid to compaction of AC due to its lubrication effect. Addition of GO to asphalt cement results in much better resistance to aging due to ultraviolet light. Graphene may also act as a barrier to dispersion of oxygen, resulting in reduced oxidative aging of AC [6]. Results of the limited studies to date suggest that increased resistance to cracking and environmental aging resulting in a much longer lifespan of AC pavements is achievable via graphene modification. In addition, creation of multifunctional asphalt pavements may be possible with graphene modification. Thermally and electrically conductive pavement could enable thermal de-icing, self-sensing for structural health monitoring, and even energy harvesting. For concrete, addition of GnP in

very low dosage rates of less than 0.005% by mass have shown a 65% increase in compressive strength and an 80% increase in flexural strength at 28 days. Reductions in resistivity and permeability of PCC were also observed, which have significant implications for improved durability of embedded steel reinforcement. Greatly reduced permeability of PCC is significant in water-retaining structures, as well as improving the overall durability of PCC in outdoor exposure applications.

The aim of this work was to demonstrate the influence of graphene properties on the ability to enhance the performance of a range of conventional materials. This paper briefly describes the potential for graphene in military water filtration systems, and improved durability and strength of assets for Force Projection.

2.0 APPROACH

2.1 Materials

2.1.1 Aqueous Contaminants

Microcystin-LR (MC-LR) standards were purchased from Eurofins Abraxis (Warminster, PA). The methanol and ultra-pure water reagents were High-Performance Liquid Chromatography (HPLC) grade and purchased from Sigma-Aldrich (St. Louis, MO). The MC-LR stock solution was prepared at a concentration of 1500 ug/L in ultra-pure water containing 10% (v/v) methanol. Diethyl phthalate (DEP) standards were purchased from Sigma-Aldrich. DEP standard solutions were prepared in HPLC grade water at 100 mg/L. Trinitro toluene (TNT) standards were obtained from undisclosed military installations.

2.1.2 Asphalt and Cementitious Materials

Commercially available standard performance grade (PG) 67-22 paving bitumen and styrene-butadiene-styrene (SBS) conventionally modified (PG 76-22) paving bitumen were obtained from Ergon Asphalt and Emulsions (Vicksburg, MS). Barite World BF-103 graphite was used for cementitious materials experiments.

2.1.3 Carbon Materials

Commercial carbon materials were used. Coconut shell Granular Activated Carbon (GAC) from Applied Membranes Inc. (Vista, CA) was evaluated with kinetic and isotherm experiments. C750 (750 m^2/g) grade graphene nanoplatelets (GnPs) from XG Sciences (Lansing, MI) were evaluated for kinetic and isotherm experiments. C500, C300, H5, H15, H25, R7, R10, R25, M5, M15, and M25 grade GnPs from XG Sciences were used in addition to C750 for asphalt experiments.

2.2 Analytical Methods

2.2.1 Detection Techniques

Microcystins-ADDA ELISA kits were purchased from Eurofins Abraxis (Warminster, PA). ELISA tests were performed according to the manufacturer's instructions for MC-LR quantification. DEP was detected using HPLC-UV using a modified method based on Thermo Scientific Application Note 1045 [7]. The column used was an Acclaim C30, 3 µm, 3.0 × 150 mm analytical column. Injection volume was 5 µL, temperature was 30°C, and UV monitoring was taken at 228 nm. The solvent gradient was as follows: 0 min 40%HPLC grade water:60% methanol; 10 min 60%water:40%methanol. There was a five-minute equilibration period between samples. TNT was detected using HPLC-UV using the method described in Felt et al., 2016 [8].

2.2.2 Characterization Techniques

Scanning Electron Microscopy (SEM) measurements of Chitosan Graphene (CSG) composites were taken on a Jeol NeoScope JSM-6000 Plus in high vacuum mode at 15 kV. Samples were mounted in the desired orientation using carbon tape to secure the composite in place. For cross-sectional determination, the edges were exposed using shears, and samples were mounted on edge. All measurements were taken at 90° with respect to the mounting block surface. Images were optimized and captured using the built in NeoScope GUI.

2.2.3 Asphalt Rheological Techniques

Low service temperature rheological behaviour of asphalt bitumen was measured in accordance with ASTM D6648 at multiple test temperatures of -6, -12, -18, and -24°C. Intermediate service temperature rheological behaviour was measured in accordance with ASTM D7175 by frequency sweeps from 0.2 to 30 Hz at 25°C. High service temperature rheological behaviour was measured in accordance with ASTM D7175 at 64, 70, and 76°C to determine an equiviscous temperature for a G*/sin δ = 2.20 kPa criterion in accordance with ASTM D7643.

2.2.3 Preparation of Graphene-Cementitious Composites

The graphene used in the preparation of graphene-paste and graphene-mortar was obtained from exfoliating a BF-103 graphite. This graphene was dispersed in aqueous media using a MasterGlenium 7920, a High-Range Water Reducing Admixture (HRWRA), manufactured by Master Builders Solutions. Stabilized aqueous graphene solution was added to cement (Laboratory-Generated Graphene paste [LGG-paste]), and mortar (LGG-mortar) mixtures at graphene loadings of 0.3, 0.6, 0.9 [9] HRWRA amount varied based on the amount of graphene used and determined as a 1.84 factor of graphene (w/w). Using tap water, the water-to-cement ratio (w/c) was kept constant at w/c = 0.4. The mixtures used Type I/II cement portland cement. The graphene-cementitious composites were cast into 2-inch diameter by 4-inch tall plastic cylindrical molds and 2-inch cubical stainless-steel molds. After casting, the paste that had been forced out onto the tops of the molds was smoothed with a trowel and left in moist for curing (fog room) until 7-, 14-, or 28-day age.

2.3 Adsorption Experiments

Organic contaminant adsorption capacities and mechanisms of two carbon materials (C750 GnPs and GAC) were assessed in batch kinetic and isotherm adsorption studies. All studies were conducted at room temperature (25 °C). Samples were collected in 1 mL aliquots at preset time points and filtered using 0.45 µm PVDF filters to remove the carbon material from solution.

2.3.1 Kinetic Experiments

For all the kinetic experiments, samples were mixed on an orbital shaker set to 120 rpm at room temperature 24 hours. The experimental results were analyzed using the linearized versions of the pseudo-first-order and pseudo-second-order kinetic models.

2.3.1.1 MC-LR Experiments

MC-LR kinetic experiments were performed with a material dosage of 50 mg/L and MC-LR concentration of 1,600 µg/L for GnP, and material dosage of 2,500 mg/L and MC-LR concentration of 1,000 µg/L for GAC. The experiment was performed by adding the carbon materials to 200 mL of MC-LR stock solution (1,000 µg/L for GAC and 1,600 µg/L for GnP). After the experiment, samples were transferred to 1.5 mL borosilicate glass vials and stored at -4ºC.

2.3.1.2 DEP and TNT Experiments

DEP and TNT kinetic experiments were performed with a material dosage of 300 mg/L and DEP or TNT concentration of 100 mg/L for both GnP and GAC. The experiments were performed by adding the carbon materials to 50 mL of either DEP or TNT stock solution. Samples were stored in 1.5 mL borosilicate glass vials and stored at 4°C while waiting for analysis.

2.3.2 Isotherm Experiments

The isotherm experiments were carried out to determine the adsorption capacity and the effect that changing the initial carbon material dosage had on contaminant adsorption. Samples were taken initially and at 24 hours to ensure removal had reached equilibrium. The experimental results were analyzed using the Langmuir and Freundlich isotherm models, where the best fit was determined using the determination coefficients (R^2) for all data.

The MC-LR experiments were performed using initial dosages of 5-50 mg/L for GnPs and 500-5,000 mg/L for GAC, keeping the initial concentration of MC-LR static at 1,600 µg/L for GnP and 1,000 µg/L for GAC. The DEP experiments had an initial dosage of 100-600 mg/L for GnP and GAC, with the initial concentration of DEP held constant at 100 mg/L. The TNT experiments were performed with initial dosages of 100 – 500 mg/L of both GnP and GAC, with the initial concentration of 100 mg/L TNT held constant.

2.4 Asphalt Accelerated Aging Experiments

Asphalt bitumen dosed with GnP was subjected to accelerated aging in accordance with ASTM D2872 (163°C for 85 min) to simulate aging during pavement production. Additional material was aged by D2872 followed by ASTM D6521 (2.1 MPa and 100°C for 40 hrs) to simulate long term environmental aging that occurs during a pavement's lifespan.

2.5 Cementitious Materials' Mechanical – Unconfined Compressive Strength – Test

Upon curing the materials in the cylinders and molds, unconfined compressive strength testing was conducted at room temperature.

The American Society for Testing and Materials, ASTM C39/C39M-21 was used in testing the cylinders [10]. To test the cubes, ASTM C109/C109M-21 was used [11]. Mechanical tests were performed immediately after taking the samples out of the fog room.

3.0 RESULTS

3.1 Graphene Characterization

SEM images of GAC and GnP from Roberts et al., 2023 are shown in Figure 1 [4]. In (a) to (c), GAC is shown to have more crevices and microporous regions than GnP in (d) to (f). GnP shows agglomeration, with a more mesoporous morphology that is advantageous for interactions with large molecules. Additionally, this type of GnP was chosen because it has a similar surface area to the compared GAC.[4] The morphology, surface area, and π networks of GnP led to interest in testing for adsorption experiments.

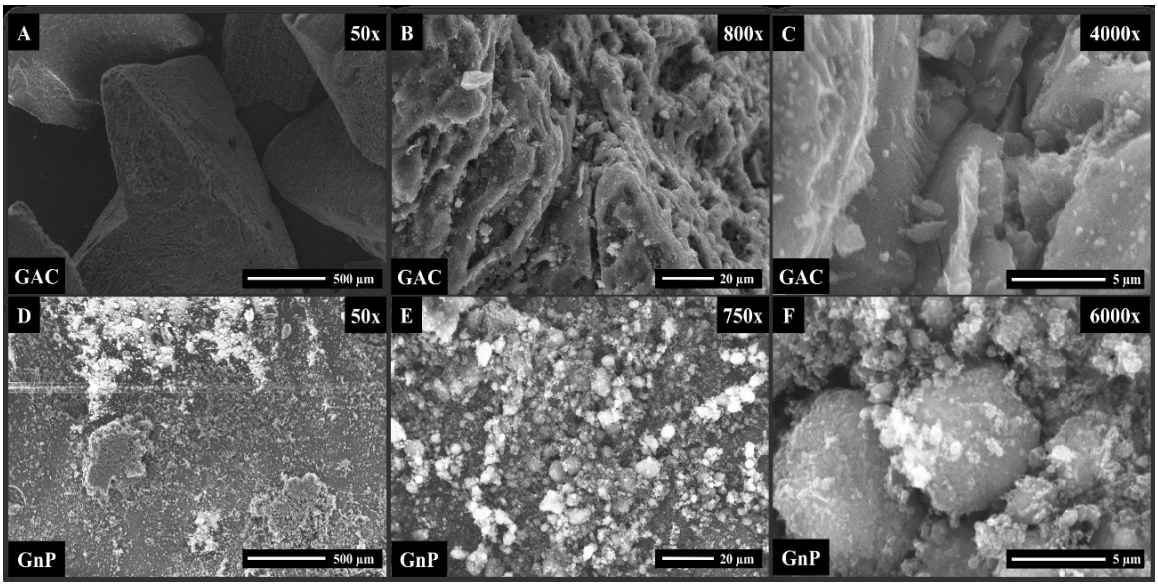

Figure 1: SEM images for GAC (a) – (c) and GnP (d) – (f).

3.2 Adsorption Study

3.2.1 Kinetic Experiments

The adsorption kinetic experiments were performed to compare and evaluate the adsorption rates and provide insight into the mechanism of interaction between aqueous contaminants and either C750 GnP or GAC. C750 GnP was selected for this treatment application due to its high surface area and availability to engage in π-π interactions with aqueous contaminants. The kinetic plots for MC-LR, DEP, and TNT are shown in Figure 2. After fitting the data to linearized pseudo-first-order ad pseudo-second-order models, results of the study including the kinetic rates were calculated and are included in Table 2.

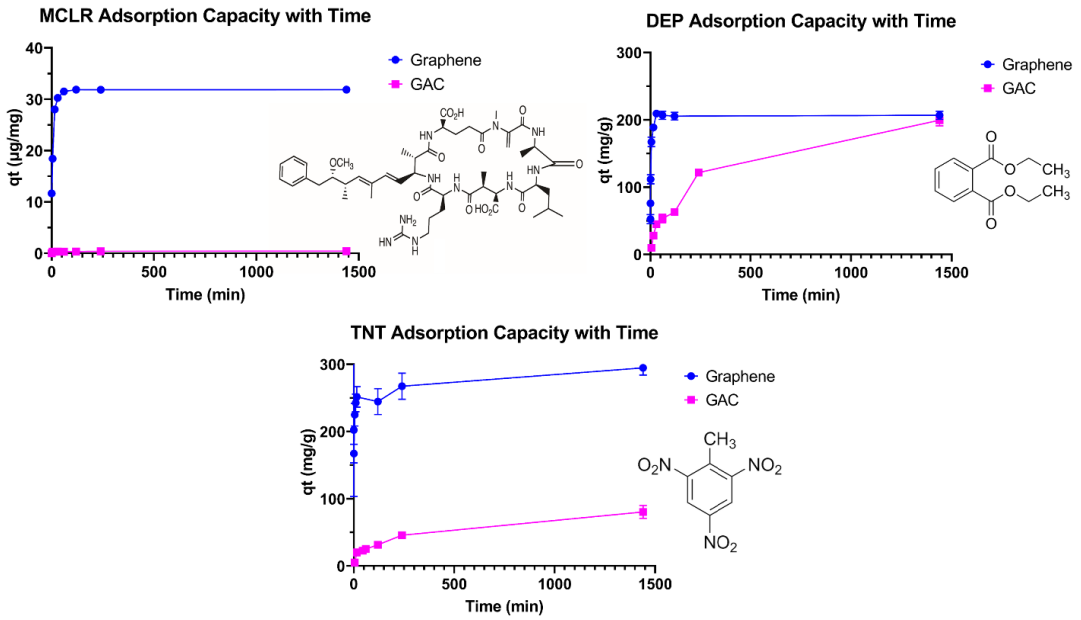

Figure 2: Kinetic 1 Plots for MC-LR, DEP and TNT.

Table 1: Kinetic Model Parameters for MC-LR, DEP and TNT.

Adsorbate	Material	Pseudo-First Order			Pseudo-Second Order		
		$Q_{e,exp}$ (mg/g)	K_1 (min^{-1})	R^2	$Q_{e,exp}$ (mg/g)	K_2 (g/mg-min)	R^2
TNT	GnP	251.5	0.088	0.722	250.0	0.013	0.998
	GAC	95.96	7E-4	0.958	100.0	5.93E-5	0.996
DEP	GnP	209.3	0.3173	0.9652	212.8	0.0046	0.9980
	GAC	217.6	0.0005	0.8140	222.1	2.88E-5	0.9988
MC-LR	GnP	0.578	262.4	0.348	42.7	0.871	1.00
	GAC	0.007	0.980	0.999	0.945	0.088	0.982

The pseudo-second-order model was the most suitable in all cases for describing both GnP and GAC kinetic data based on the R^2 values. The adsorption of all contaminants to GnP was the fastest process, being complete within 30 minutes, whereas GAC required 4 hours to reach equilibrium. When comparing k_2 values, GnP values are 2-3 orders of magnitude higher than k_2 values for GAC for the same contaminant. This is advantageous for treatment applications, because it allows shorter residence time in a graphene treatment system than a GAC treatment system. As a result, graphene treatment systems can be smaller, allowing for a lower footprint in locations with space restrictions, or during operations with high mobility requirements.

3.2.2 Isotherm Experiments

Equilibrium isotherm model analysis for GnP and GAC was completed and fitted to the experimental results for further understanding of the adsorption capacities and mechanisms.

Table 2: Isotherm Model Results for MC-LR, DEP and TNT.

Adsorbate	Material	Langmuir			Freundlich				Capacity Results
		R_L	Q_m (mg/g)	R^2	K_F ((mg/g)(L/mg))$^{1/n}$	1/n	Q_m (mg/g)	R^2	Qe,max,calc (mg/g)
TNT	GnP	0.051	366.2	0.989	138.3	0.278	338.3	0.996	338.3
	GAC	-0.015	96.98	0.960	131.1	0.041	150.8	0.184	96.98
DEP	GnP	0.007	184.3	0.993	133.6	0.087	179.7	0.635	184.3
	GAC	0.067	166.4	0.9904	40.1	0.2336	88.7	0.9209	166.4
MC-LR	GnP	0.578	262.4	0.348	42.7	0.871	130.9	0.974	130.9
	GAC	0.007	0.980	0.999	0.945	0.088	0.973	0.982	0.980

When comparing the R^2 values for Langmuir vs Freundlich model, Langmuir better models the behaviour of GAC for all contaminants. Freundlich is the representative model for GnP for TNT and MC-LR, while Langmuir better represents GnP removal for DEP. In all cases, the calculated adsorption capacity for GnP is higher than for GAC, and in the case of MC-LR, is more than two orders of magnitude higher. This demonstrates that graphene is a better adsorbent for certain compounds than traditional water treatment techniques like GAC. The presence of π-π interactions and a more mesoporous structure than GAC allows GnP to be selectively chosen for treatment applications in which large, π rich molecules are present.

3.3 Asphalt Bitumen Aging

The flexibility of asphalt bitumen is detrimentally affected by aging, which leads to cracking and other forms of deterioration for AC in service (Figure 3a). Low temperature rheological data was interpreted to determine the number of hours of accelerated aging required to induce an equivalent level of flexibility in each bitumen tested. This is directly related to the potential for cracking of the material. Figure 3b presents the results for some of the best performing GnP modified bitumen materials and includes the SBS polymer modified bitumen for comparison. The SBS modified bitumen shows a 51% improvement relative to the unmodified bitumen; this data aligns with the proven cracking resistance improvements observed for polymer modified AC in large scale field trials [12]. By comparison, the data shows improvements greater than 150% compared to unmodified bitumen for the GnP modified bitumen. This potentially represents a significant additional level of improvement in cracking resistance if the behaviour is found to translate to field behaviour of AC.

Intermediate temperature results for aged bitumen are provided in Figure 3c. A higher phase angle at the threshold stiffness of 8.967 x 10^{-6} Pa represents better flexibility. All of the modified bitumen materials have improved flexibility relative to the unmodified bitumen, but the effect of GnP modification is less dramatic compared to that of SBS polymer modification. High temperature stiffness results for the aged bitumen are presented in Figure 3d. Higher values represent improved resistance to rutting deformation under traffic. The GnP modified bitumen materials have lower effect than the SBS polymer modified bitumen, but do not cause any detrimental effects relative to the unmodified base bitumen.

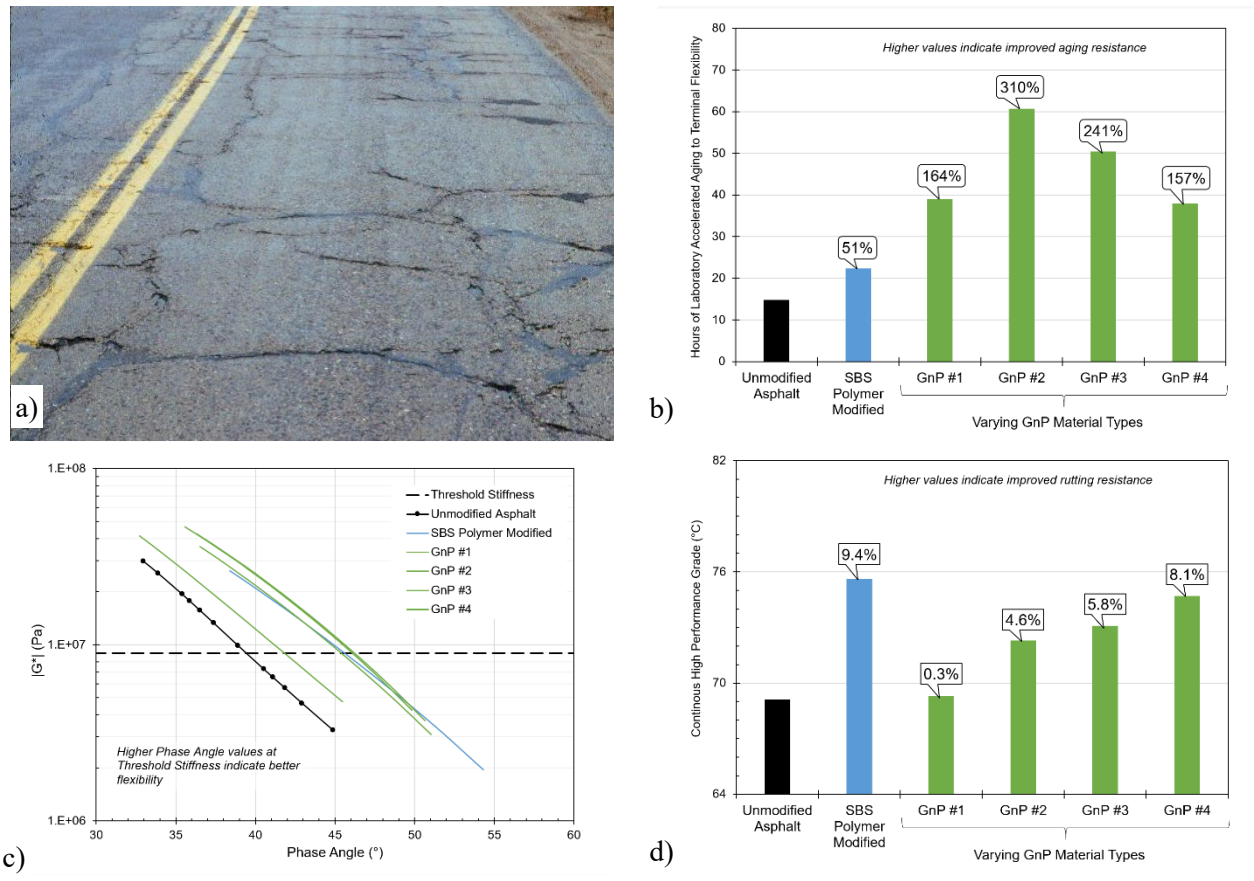

Figure 3: Asphalt Results: (a) aging deterioration of a roadway; (b) low temperature flexibility; (c) intermediate temperature flexibility; (d) high temperature stiffness.

3.4 Cement Paste and Mortar Compressive Strength

Three samples for each different graphene loading were tested for compressive strength. Average and maximum compressive strength results were compared to understand the trends in these LGG-cementitious materials. Figure 4 and Figure 5 show the maximum compressive strength results for LGG-paste and LGG-mortar, respectively. These figures were plotted against curing days and $r_{strength}$, which represents the maximum compressive strength of LGG composites compared to the reference materials without the graphene. The samples were cured for 7, 14, and 28 days. The compressive strengths of the samples were measured at the end of each curing cycle and the compressive strength increased as a function of curing time except for one graphene dosage (0.3%). The increase was more significant in LGG-mortar samples due to the presence of existing interfacial charge transition zone (ITZ), providing better interaction between the graphene and cementitious phase compared to LGG-paste in determining the mechanical properties of composites. Both materials presented an optimum graphene loading that resulted in better dispersion and higher compressive strength. Additionally, it was observed that graphene accelerated the hydration kinetics in both cementitious materials. This resulted in minimized or reduced compressive strength increase at the 28th day compared to 7 and 14 days compared to reference materials.

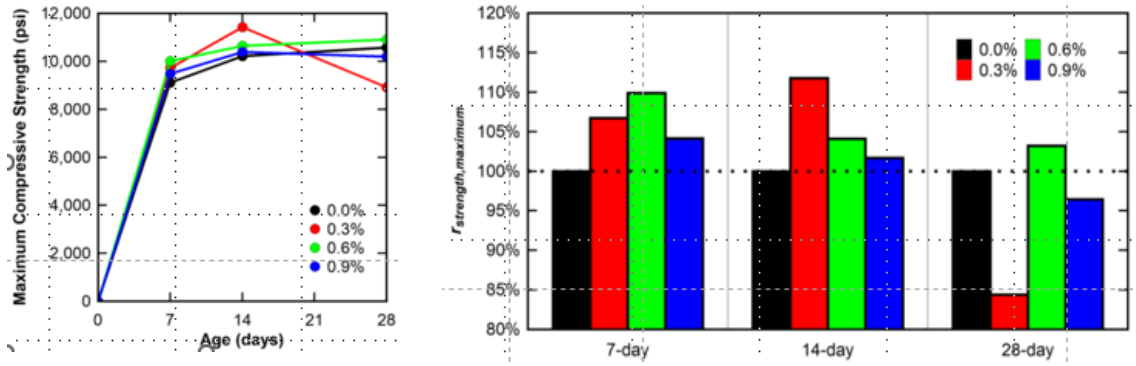

Figure 4: Compressive strength results for LGG-paste.

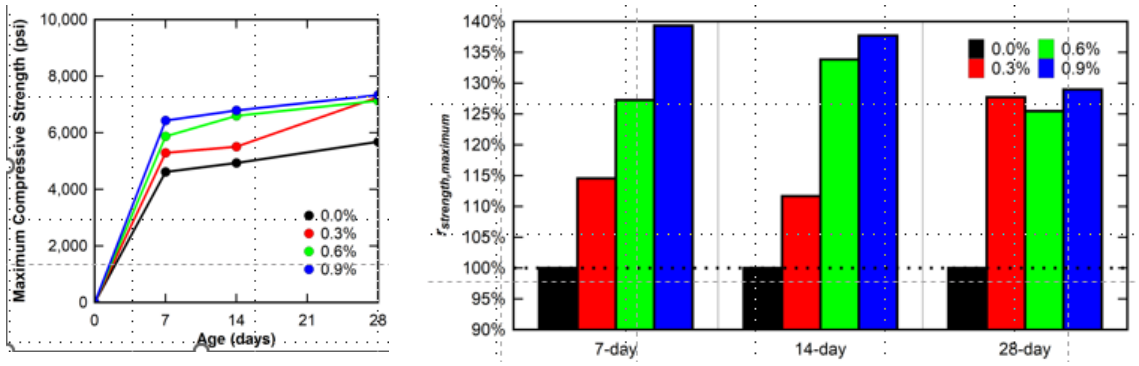

Figure 5: Compressive strength results for LGG-mortar.

4.0 CONCLUSIONS

Due to the multifunctional nature of graphene, the aim of this work was to investigate the influence of graphene properties on the ability to enhance the performance of a range of conventional materials. By selecting the size, surface area, and morphology for the desired application, significant performance gains were realized for the capacity and kinetics to remove the following: Endocrine Disruptors (EDC), hepatotoxin (MC-LR) from a

metabolite of cyanobacteria, and an explosive munition compound TNT. This novel materials-based approach for water security can be applied to the wide range of aromatic contaminants found in water sources found in military environments.

In addition to materials and technologies for water security and chemical adsorption/filtering; enhanced bitumen and cement formulations were realized. For asphalt applications, SBS modified bitumen shows a 51% improvement relative to controls aligning with the proven cracking resistance improvements observed for polymer modified AC at scale. The data also shows improvements greater than 150% compared to unmodified bitumen for the GnP modified bitumen. This potentially represents a significant additional level of improvement in cracking resistance. The presence of graphene in cementitious materials increased the compressive strength of LGG-paste and mortar by 12% to 38%, respectively, compared to their reference materials. The existence of ITZ region of the LGG-mortar samples was found to have a big impact on the mechanical strength of materials. Graphene-accelerated cement hydration during the first 14 days of curing. This resulted in increased compressive strength compared to reference. However, after 28 days of curing, the LGG-paste samples did not offer significant improvement over the reference, and in one sample the compressive strength diminished considerably. The compressive strengths of the LGG-mortar samples increased about 25% on average regardless of the graphene dosage.

These results suggest that the inherent properties of graphene can provide the ideal structure and compatibility for a novel molecular approach to enhance material performance. It is anticipated that these findings will guide the design of demonstrations in simulated operational environments, producing useful logistical and life cycle savings for Force Projection that enable the potential for significant cost reductions and operational readiness. for mobilization and maintenance costs

5.0 ACKNOWLEDGEMENTS

The authors would like to thank the 6.3 Military Engineering Graphene for Military Applications Program for funding.

6.0 REFERENCES

[1] Amadei, C.A., and Vecitis, C.D., How to increase the signal-to-noise ratio of graphene oxide membrane research. J Phys Chem Lett, 7(19) 3791-3797. 2016. https://doi.org/10.1021/acs.jpclett.6b01829

[2] US CHPPM. Medical surveillance monthly report. US CHPPM. 2001.

[3] TB Med 577: Sanitary control and surveillance of field water supplies. 2005

[4] Roberts, J.L., Graphene as a rational interface for enhanced adsorption of microcystin-LR from Water. Hazardous Materials. In press. 2023.

[5] Lattao, C., Cao, X., Mao, J., Schmidt-Rohr, K., Pignatello, J.J., Influence of molecular structure and adsorbent properties on sorption of organic compounds to a temperature series of wood chars. Environ Sci Technol, 48(9) 4790-8. 2014. https://doi.org/10.1021/es405096q

[6] He, J., Hu, W., Xiao, R., Wang, Y., Polaczyk, P., Huang, B., A review on graphene/GNPs/GO modified asphalt. Construction and Building Materials, 330. 2022. https://doi.org/10.1016/j.conbuildmat. 2022.127222

[7] Jing, C., Qun,. X, Rhorer, J., Determination of phthalates in drinking water by UHPLC with UV detection. T. F. Scientific (Ed.), (Vol. 1045).

[8] Felt, D., Gurtowski, L., Nestler, C.C., Johnson, J., Larson, S., A two-stage extraction procedure for insensitive munition (IM) explosive compounds in soils. Chemosphere, 165 18-26. 2016. https://doi.org/10.1016/j.chemosphere.2016.08.098

[9] Ucak-Astarlioglu, M.G., Graphene in cementitious materials for military applications. In press. 2023.

[10] ASTM C39/C39M-21 Standard test method for compressive strength of cylindrical concrete specimens. ASTM. 2021.

[11] ASTM C109/C109M-21 Standard test method for compressive strength of hydraulic cement mortars (Using 2-in. or [50 Mm] cube specimens). ASTM. 2021.

[12] Von Quintus, H.L., Mallela, J., Buncher, M., Von Quintus, H.L., Mallela, J., Buncher, M., Quantification of effect of polymer-modified asphalt on flexible pavement performance. Journal of the Transportation Research Board, 141-154. 2001. https://doi.org/DOI: 10.3141/2001-16.